FEBS Letters 584 (2010) 625–630

journal homepage: www.FEBSLetters.org

Glyceraldehyde-3-phosphate dehydrogenase tetramer dissociation and amyloid fibril formation induced by negatively charged membranes

Leonardo M. Cortez, César L. Ávila, Clarisa M. Torres Bugeau, Ricardo N. Farías, Roberto D. Morero, Rosana N. Chehín *

Departamento Bioquímica de la Nutrición, Instituto Superior de Investigaciones Biológicas (CONICET-UNT), Chacabuco 461 (4000), Tucumán, Argentina
Departamento Bioquímica de la Nutrición, Instituto de Química Biológica Dr. Bernabé Bloj, Chacabuco 461 (4000), Tucumán, Argentina

ARTICLE INFO

Article history:
Received 21 October 2009
Revised 2 December 2009
Accepted 9 December 2009
Available online 13 December 2009

Edited by Jesus Avila

Keywords:
Glyceraldehyde-3-phosphate dehydrogenase
Infrared spectroscopy
Protein–membrane interaction
Amyloid

ABSTRACT

Glyceraldehyde-3-phosphate dehydrogenase (GAPDH) is a multifunctional enzyme related with Huntington's, Parkinson's and Alzheimer's diseases. The ability of negatively charged membranes to induce a rapid formation of GAPDH amyloid fibrils has been demonstrated, but the mechanisms by which GAPDH reaches the fibrillar state remains unclear. In this report, we describe the structural changes undergone by GAPDH at physiological pH and temperature conditions right from its interaction with acidic membranes until the amyloid fibril is formed. According to our results, the GAPDH-membrane binding induces a β-structuring process along with a loss of quaternary structure in the enzyme. In this way, experimental evidences on the initial steps of GAPDH amyloid fibrils formation pathway are provided.

1. Introduction

Glyceraldehyde-3-phosphate dehydrogenase (GAPDH) is a well-studied protein for its role in cellular energy production as a glycolytic enzyme. However, current evidences reveal that this enzyme is actually a multifunctional protein displaying a number of diverse cellular functions unrelated to glycolysis [1]. These functions include transcription activation [2], metabolic switch between the cytosol and the nucleus linking the metabolic state to the gene transcription [3], membrane fusion [4], microtubule bundling [5], and apoptosis through its binding to DNA as a transcription activator. GAPDH is also implicated in some neuronal diseases. In fact, immunofluorescence analysis revealed that GAPDH is co-localized with α-synuclein in Lewy bodies on Parkinsońs disease [6] and drugs that are currently in use for treatment bind to or affect GAPDH function [7]. Moreover, several studies have shown that GAPDH is located in amyloid plaques [8,9] and binds the amyloid precursor protein [10] and Aβ peptide [11], indicating that GAPDH might play a role in the progression of Alzheimeŕs disease. In vitro, oxidants can induce amyloid-like aggregation of GAPDH via the formation of intermolecular disulfide bonds [12]. At physiological conditions of pH and temperature, GAPDH is capable to undergo strong conformational changes from globular soluble to β-sheet enriched amyloid structure when they interact with membranes containing anionic phospholipids [13]. The fibrils formed under this conditions appear to be analogous to those isolated in vivo [13], and hence this system constitutes a good model to study the molecular basis of amyloid fibril formation in vitro.

In the present work, kinetics and structural analysis were performed in order to detect the changes undergone by the enzyme upon its binding to negatively charged membranes. Our experimental evidences allow us to suggest that a β-structuring and tetramer dissociation processes occurs prior to the appearance of protein aggregates. The results presented herein offers novel insight into the initial steps of the amyloid fibrils formation pathway.

2. Materials and methods

2.1. Materials

Glyceraldehyde-3-phosphate dehydrogenase (EC 1.2.1.12) and Thioflavin T (ThT) were purchased from Sigma–Aldrich (St. Louis, MO). Dioleylphosphatidylcholine (DOPC) and dioleylphosphatidic acid (DOPA) were obtained from Avanti Polar lipids and their purity controlled by TLC.

* Corresponding author. Address: INSIBIO, Chacabuco 461 (4000), Tucumán, Argentina. Fax: +54 381 4248921.
E-mail address: rosana@fbqf.unt.edu.ar (R.N. Chehín).

0014-5793/$36.00 © 2009 Federation of European Biochemical Societies. Published by Elsevier B.V. All rights reserved.
doi:10.1016/j.febslet.2009.12.012

2.2. Vesicles preparation

Small unilamellar vesicles (SUV) were prepared according to Finer [14]. Briefly, appropriate amounts of DOPC and DOPA were dissolved in chloroform/methanol (2:1, vol/vol) and dried under nitrogen. The lipids were rehydrated in the appropriate buffer and sonicated on ice under nitrogen with a probe-type sonifier. Cycles of sonication (1 min) and cooling (1 min) were repeated up to 15 times until the initially cloudy lipid dispersion became translucent. The suspension was centrifuged for 15 min at 1100×*g* to obtain a pure SUV suspension.

2.3. GAPDH enzymatic activity assay

GAPDH enzymatic activity was measured following the increase in the absorbance at 340 nm of NADH using a Beckman DU-7500 spectrophotometer. Briefly, 0.16 mg/ml of GAPDH in the presence or in the absence of 0.5 mM DOPC:DOPA (9:1) liposomes were incubated at 37 °C, pH 7.4. Afterwards, the enzymatic reaction was carried out at 25 °C and was initiated by the addition of a 20 μl aliquot of the previous suspension to a reaction mixture containing 100 mM glycine, 100 mM Na_2HPO_4, 5 mM EDTA, 1.5 mM NAD and 2 mM glyceraldehyde-3-phosphate at pH 9.0.

2.4. Hydrogen–deuterium exchange measurement

The lyophilized protein was dissolved in 50 μl of deuterated buffer alone or containing 12.5 mM of DOPC:DOPA liposomes and immediately mounted into an IR cell with a path length of 100 μm. The infrared spectra were recorded every minute up to 180 min. Sixteen scans were collected for each time interval. To compare the spectra in H_2O and D_2O, they were normalized using the amide I band in H_2O to the amide I band in D_2O at 1 min as reference. The spectrum collected after exchange for 24 h was used as the fully deuterated spectrum.

2.5. Amide proton exchange rate

The H–D exchange of GAPDH was followed by FT-IR measuring the apparent intensity changes of the amide II band, located around 1548 cm^{-1} [15]. The fraction of unexchanged amide proton, *F*, was calculated at various time intervals as follows:

$$F = (A_I - A_{II\infty})/A_I\omega$$

where A_I and A_{II} are the maximum absorbance of the amide I and II bands, respectively, $A_{II\infty}$ is the amide II maximum absorbance of fully deuterated protein, and ω is the ratio of A_{IIo}/A_{Io}, with A_{IIo} and A_{Io} being the maximum absorbance for the amide II and amide I bands, respectively, of GAPDH in H_2O [16].

2.6. Thioflavin T fluorescence measurements

Eighty microliters of a GAPDH (4 mg/ml) solution were mixed with 2 ml of 20 mM HEPES, pH 7.4, containing 25 μM ThT and incubated at 37 °C in the presence or in the absence of 0.5 mM of DOPC or DOPC:DOPA (9:1, 8:2 or 7:3 molar ratios) liposomes in a quartz cuvette. The scattering, measured in the absence of ThT, was subtracted. All fluorescence measurements were carried out with an ISS (Champaign, IL, USA) PC1 spectrofluorometer according to Levine et al. [17]. The excitation wavelength was set at 450 nm with emission measured at 482 nm using a slit width of 0.5 and 1 nm for excitation and emission light paths respectively. Each experiment was conducted in triplicate.

2.7. Fourier transform infrared spectroscopy measurements

GAPDH solutions for infrared studies were prepared in 20 mM HEPES, pD 7.4. Around 50 μl of sample containing 4 mg/ml of GAPDH were assembled in a thermostated cell between two CaF_2 windows with 100 μm spacers in a demountable liquid cell (Harrick Scientific, Ossining, NY). The samples were recorded in a Nicolet 5700 spectrometer equipped with a DTGS detector (Thermo Nicolet, Madison, WI). The sample chamber was permanently purged with dry air. Solvent subtraction, deconvolution, determination of band position and curve fitting of the original amide I band were performed as previously described [18]. Protein structural analyses, either in the absence or in the presence of the liposomes were repeated three times with fresh new samples to test the reproducibility of the measurements. In all cases, the differences among the three experiments were lower than 3%. The error in estimation of the percentage of secondary structure depends mainly on the removal of spectral noise, and it was estimated to be 2% [19].

2.8. Transmission electron microscopy

GAPDH (4 mg/ml) solution in 20 mM HEPES, pH 7.4, were mixed with 12.5 mM of DOPC and DOPC:DOPA (9:1) during 120 min. The samples were primary fixed in Karnovsky fixative buffer. After 3 h at 4 °C, pellets were embedded in agar-agar and transferred to 1% osmium tetroxide overnight. After rinsed in distilled water, the sample was treated with an aqueous solution of 2% uranyl acetate for 40 min. After fixation, samples were gradually dehydrated in alcohols of increasing strength, followed by acetone. The infiltration with the embedding medium was performed in Spurr resin (Pelco Int., CA, USA). Ultrathin sections mounted on copper grids were stained with uranyl acetate and examined with a Zeiss EM 109 transmission electron microscope.

3. Results

3.1. Lipid-induced conformational changes in GAPDH

The glycolytic activity of GAPDH in the presence of acidic membranes shows an exponential decay over time (Fig. 1A). On the contrary the enzyme preserves its activity while incubated in the absence of liposomes.

In order to test for structural rearrangements on GAPDH induced by acidic liposomes, the H–D exchange rate was followed by infrared spectroscopy. The kinetics of the process in the absence or presence of DOPC:DOPA (9:1) liposomes was fitted to a two-exponential decay model (Fig. 1B) which was satisfactorily used in other systems [20,21] . Because of the complexity of the overall H–D exchange process in proteins, only qualitative analyses were performed. The amount of amide protons exchanged in the presence of acidic liposomes is significantly higher and the overall process faster than in its absence. These data suggest that conformational changes occur with the exposition of new protein solvent accessible surfaces. The main changes in the H–D exchange takes place within the first 5 min of protein–membrane interaction.

3.2. Kinetics of lipid-induced GAPDH amyloid fibrils formation

The ability of GAPDH to form amyloid fibrils in the presence of acidic membranes was investigated through monitoring maximal ThT emission intensity over 80 min of incubation at 37 °C and shown in Fig. 2A. In the presence of DOPC:DOPA (9:1) membranes, the aggregation kinetics shows a lag phase (10 min) followed by an exponential phase which corresponds to the amyloid fibril elongation. The amount of negative charge in the bilayer increases the ex-

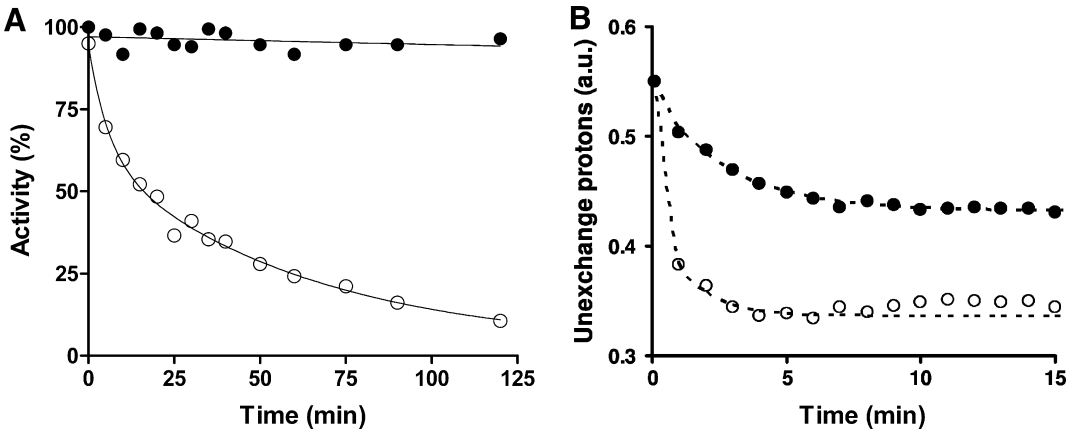

Fig. 1. Glycolytic activity (A) and amide I proton exchange rates in D_2O (B) for GAPDH in the absence (filled circles) or in the presence (empty circles) of DOPC:DOPA (9:1) liposomes at 37 °C, pH 7.4. The lines represent best fits to the data points.

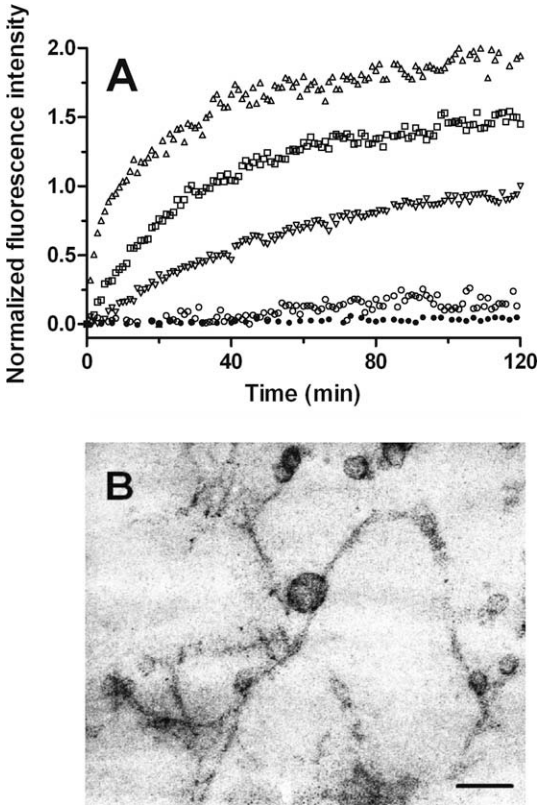

Fig. 2. (A) Kinetics of lipid-induced GAPDH amyloid fibrils formation. The ThT fluorescence emission of a 0.16 mg/ml GAPDH solution in the absence (filled circles) or in the presence of 0.5 mM DOPC (empty circle). 9:1 (inverted triangle), 8:2 (square), 7:3 (triangle) DOPC:DOPA liposome's suspension registered as a function of time. (B) Lipid-induced GAPDH fibrils observed by transmission electronic microscopy. GAPDH solution (4 mg/ml) was incubated at 80 min 37 °C of incubation in the presence of 12.5 mM DOPC:DOPA (9:1) suspension. The scale bars at the bottom correspond to 100 nm.

tent of GAPDH amyloid fibrils formation and shortens the lag phase. Fig. 2B shows the fibrilar nature of the aggregates as well as large unilamellar liposomes formed as a consequence of the fusogenic activity previously described for GAPDH [4].

In the absence of liposomes, as well as in the presence of zwitterionic membranes, the protein kept its soluble state and no considerable amount of amyloid fibrils was detected.

3.3. Characterization of the GAPDH structural changes induced by acidic membranes

In order to characterize the structural rearrangement undergone by GAPDH in the presence of acidic membrane, infrared spectroscopy analyses were performed (Fig. 3 and Table 1) using DOPC:DOPA (9:1) membranes since a 10 min lag phase allows structural changes measurements before the fibrillation process begins. After 80 min of incubation at 37 °C, GAPDH remained stable and no changes in amide I spectra were observed (Fig. 3A). The dominant band at 1654 cm^{-1} reflects the content of α-helical while the band component at 1638 cm^{-1} indicates the presence of β-sheet with some contributions from non-structured conformations [22]. The band located around 1667 cm^{-1} arises from β turns [23,24]. The band at 1681 cm^{-1} may also arise from a small contribution of the high-frequency vibration of the antiparallel β-strand [23]. Bands appearing at about 1642 cm^{-1} are assigned to non-structured conformation [22]. The band at 1623 cm^{-1} corresponds to interoligomeric contact as will be described in the following section. According to the band assignment given above, the GAPDH structure consists of 30% α-helix, 29% β-sheet, and 11% β-turns (Fig. 3B and Table 1). This secondary-structure content is in good agreement with those obtained by X-ray analysis [25].

After 80 min of incubation at 37 °C in the presence of DOPC:DOPA liposomes, significant structural changes on the protein were evidenced along with the emergence of a new band corresponding to protein aggregation at 1616 cm^{-1} [18]. In this way, it is notable the increase of the β-sheets, β-turns and aggregation bands, while β-helix and interoligomeric bands diminished (Fig. 3C and Table 1). In addition, the contribution from random coil becomes almost undetectable. In accordance with the observations derived from fluorescence assays, upon incubation with DOPC liposomes the protein kept its soluble state and no considerable amount of amyloid fibrils was detected (data not shown).

3.4. Identification of GAPDH interoligomeric contact band

Bands in the 1630–1600 cm^{-1} region are not common in native proteins. The band at 1623 cm^{-1} has been assigned to protein–protein contacts in native oligomeric proteins as well as β-strands not forming β-sheets [18,26]. Considering that GAPDH can be dissociated into dimmers or monomers at 45 °C [27], the thermal tetramer dissociation was studied by infrared spectroscopy in order to achieve an unmistakable assignment of the 1623 cm^{-1} band. Fig. 4 shows that this band diminishes with increasing temperature until it vanishes at 50 °C, which strongly suggests that it arises

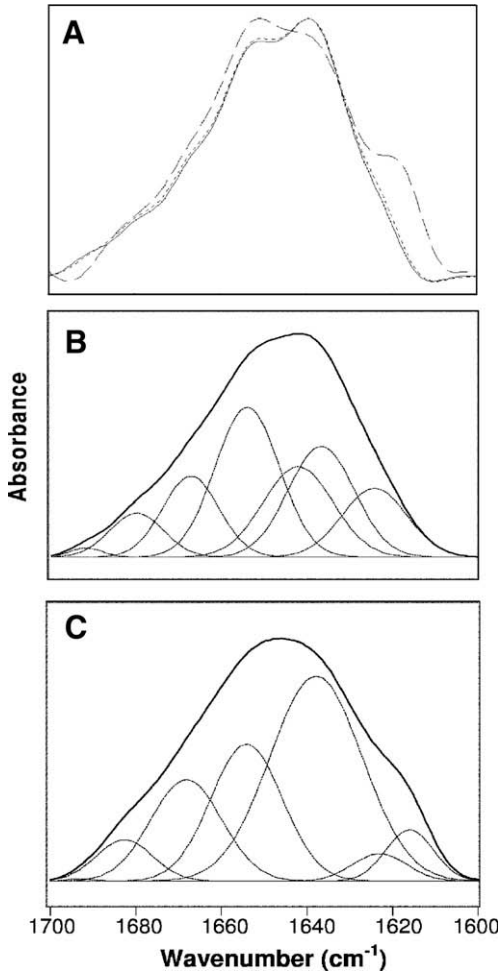

Fig. 3. (A) FT-IR absorption spectra in the amide I region GAPDH before (solid line) and after 80 min of incubation at 37 °C in the absence (dotted line) and in the presence (dashed lines) of 12.5 mM DOPC:DOPA (9:1) liposomes. Reconstruction of the amide I band from the components at 37 °C before (B) and after 80 min of protein–membrane interaction (C).

Table 1
Band position (cm^{-1}) and percentage area (%) corresponding to the components obtained after curve fitting of the GAPDH amide I band after 80 min of incubation at 37 °C in the absence and in the presence of DOPC:DOPA liposomes.

GAPDH		+DOPC:DOPA	
Position (cm^{-1})	Area (%)	Position (cm^{-1})	Area (%)
1681	8	1682	5
1667	12	1667	18
1654	29	1653	22
1642	18	1643	<1
1638	21	1637	45
1623	12	1623	3
1616	–	1616	7

from the GAPDH monomers and/or dimmer contacts. It is important to note that the GAPDH intermolecular hydrogen bonds from protein aggregation, characterized by the 1616 cm^{-1} band, becomes evident at about 45 °C, just when the tetramer is being dissociated.

3.5. Time-progression of GAPDH structural changes

A detailed time-progression of the structural changes occurred during the lipid-induced GAPDH refolding are depicted in Fig. 5.

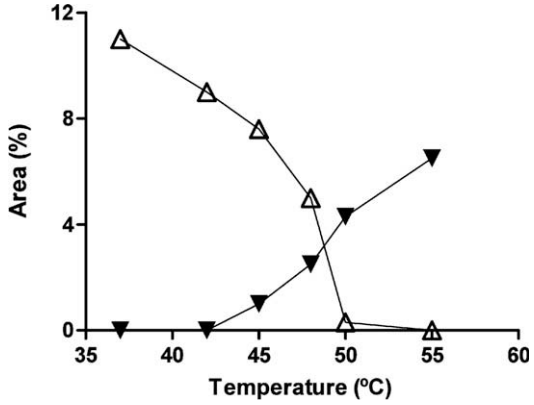

Fig. 4. Relative areas of 1623 cm^{-1} (open triangles) and 1616 cm^{-1} (filled triangles) bands obtained after curve fitting of GAPDH amide I band. The protein spectra were registered as a function of temperature. The contribution of each band to the amide I was performed according to experimental procedures.

The protein secondary structure changes derived from the infrared spectrum are shown in Fig. 5A. The main structural changes were observed during the lag phase, i.e. within the first 10 min of incubation, where the signal from β-sheet strongly increases at the expense of the unordered structure. On the contrary, the α-helix content shows a slower decrement and this process covers the lag and the amyloid fibrils growth phase. Fig. 5B shows the band areas related with interchain interaction and it seems clear that subsequent to the protein-membrane binding, the tetramer began its dissociation and the intermolecular aggregation started. It is important to take into account that in the lag phase, both, the main β-structuring and the tetramer dissociation have been almost completed (Fig. 5A and B).

4. Discussion

Independent analyses demonstrate that GAPDH might be involved in the pathogenesis of some protein misfolding diseases [28], but its precise role in neurodegenerative diseases is still unknown. The observation that the interaction of soluble Aβ peptide and denatured forms of GAPDH is rather specific and not due to its adsorption to other denatured proteins lead to the hypothesis that non-native forms of GAPDH might act as a seed in the formation of amyloid structures during Alzheimer's disease [29]. Acidic membranes can also trigger the formation of GAPDH amyloid fibrils at physiological conditions, and the formed fibrils are analogous to those found in some pathological conditions [13]. In this way, the study of the physicochemical basis of the ability of this enzyme to form amyloid fibrils acquired relevance. In the present work, the first description of the kinetics and conformational events underwent by GAPDH right from its binding to acidic membrane until the cross-β structure becomes evident is reported. The kinetic of the lipid-induced GAPDH fibrillation showed that after a short lag phase of about ten minutes, the amyloid fibrils growth phase proceeded in an exponential way. This result is consistent with a nucleation-dependent process that appears to be a common feature in some amyloid fibril formation [30]. The main conformational changes in the protein occurs within the lag phase, where a protein β-structuring was evidenced by infrared techniques. The GAPDH–DOPC:DOPA binding energy, which is about −5.09 kcal/mol [31], could be used to support the observed conformational change resembling the SNARÉs systems [32].

In this paper, it is also demonstrated that in GAPDH, the 1623 cm^{-1} band from the infrared spectrum could be unambiguously assigned to interoligomeric interaction and allows to monitoring the tetramer dissociation. According to our results,

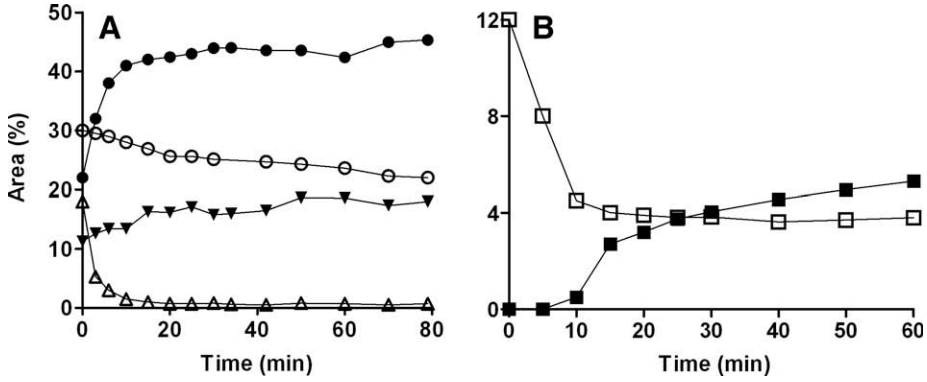

Fig. 5. Relative contribution of secondary structure (A) and interchain interaction (B) to the amide I band as a function of time. The infrared spectra were recorded after a GAPDH solution (4 mg/ml) was added to a 12.5 mM DOPC:DOPA liposome suspension. Area percentages at each time are represented for β-sheets (filled circles), α-helix (open circles), β-turns (filled triangles), random coil (open triangles), interoligomeric contact (open square) and protein aggregation (filled square).

GAPDH is being dissociated within the lag phase (Fig. 5B). This fact could explain the increment on the protein's solvent accessible area, as evidenced by the H–D exchange, which might arise from lost of the interoligomeric contacts (Fig. 1B).

According to GAPDH X-ray crystallography the interface between two monomer has an edge to edge β-sheet structure, while the dimmers pack together through loops and random coil structures [25]. Thus, when GAPDH interacts with acidic membranes, the random coil (including those belonging to the dimmer interface) could be organized into β-structures leading to the tetramer dissociation and the concomitant exposition of hydrophobic surfaces triggering the interchain aggregation. Moreover, the tetramer dissociation could also explain the loss of glycolytic activity observed in the presence of acidic membranes (Fig. 1A) since this enzymatic activity is restricted to the tetramer [33].

The first critical step in protein fibrillogenesis is the partial unfolding of the protein [34]. However, it is difficult to trap and characterize such partially folded species under physiological conditions because they are only transiently populated on the fibrillation pathway [35]. It has been assumed that conformational change from α-helix into β-sheet may be a key step in the formation of amyloid fibrils in some proteins [35]. However, according to our results, in GAPDH, the β-sheet increment is first at the expense of random coil while the α-helix unfolding seems to be a less important process.

The loss of quaternary structure and the partial interconversion of secondary structure elements detected in the lag period, allow us to characterize intermediate species in the GAPDH folding pathway. The isolation of these intermediate species is difficult due to the short duration of the lag period. This fact alongside the high light scattering produced by the presence of lipid vesicles prevents the study of these intermediates by other classical biophysical techniques. In this scenario, infrared spectroscopy becomes a useful tool.

The data presented herein provide some insights on the GAPDH misfolding pathway since intermediates folding species were experimentally detected. This could shed light on the molecular mechanisms that drive the GAPDH amyloid formation, associated with various, often highly debilitating, diseases like Alzheimer's, Parkinson's or Huntington's disease, for which no sufficient cure is available yet.

Acknowledgements

This work was supported by Consejo Nacional de Investigaciones, Agencia de Promoción Tecnológica (PAE 22642) and Secretaría de Ciencia y Técnica de la Universidad Nacional de Tucumán (CIUNT) Grant D313. The authors are grateful to Dra. Beatriz Winik for her valuable contribution with the electronic microscopy.

References

[1] Sirover, M.A. (1999) New insights into an old protein: the functional diversity of mammalian glyceraldehyde-3-phosphate dehydrogenase. Biochim. Biophys. Acta 1432, 159–184.
[2] Zheng, L., Roeder, R.G. and Luo, Y. (2003) S phase activation of the histone H2B promoter by OCA-S, a coactivator complex that contains GAPDH as a key component. Cell 114, 255–266.
[3] Hara, M.R. et al. (2005) S-Nitrosylated GAPDH initiates apoptotic cell death by nuclear translocation following Siah1 binding. Nat. Cell Biol. 7, 665–674.
[4] Morero, R.D., Vinals, A.L., Bloj, B. and Farias, R.N. (1985) Fusion of phospholipid vesicles induced by muscle glyceraldehyde-3-phosphate dehydrogenase in the absence of calcium. Biochemistry 24, 1904–1909.
[5] Huitorel, P. and Pantaloni, D. (1985) Bundling of microtubules by glyceraldehyde-3-phosphate dehydrogenase and its modulation by ATP. Eur. J. Biochem. 150, 265–269.
[6] Tatton, W.G., Chalmers-Redman, R.M., Elstner, M., Leesch, W., Jagodzinski, F.B., Stupak, D.P., Sugrue, M.M. and Tatton, N.A. (2000) Glyceraldehyde-3-phosphate dehydrogenase in neurodegeneration and apoptosis signaling. J. Neural Transm. Suppl. 77, 100.
[7] Kragten, E. et al. (1998) Glyceraldehyde-3-phosphate dehydrogenase, the putative target of the antiapoptotic compounds CGP 3466 and R-(−)-deprenyl. J. Biol. Chem. 273, 5821–5828.
[8] Sunaga, K., Takahashi, H., Chuang, D.M. and Ishitani, R. (1995) Glyceraldehyde-3-phosphate dehydrogenase is over-expressed during apoptotic death of neuronal cultures and is recognized by a monoclonal antibody against amyloid plaques from Alzheimer's brain. Neurosci. Lett. 200, 133–136.
[9] Tamaoka, A., Endoh, R., Shoji, S., Takahashi, H., Hirokawa, K., Teplow, D.B., Selkoe, D.J. and Mori, H. (1996) Antibodies to amyloid beta protein (A beta) crossreact with glyceraldehyde-3-phosphate dehydrogenase (GAPDH). Neurobiol. Aging 17, 405–414.
[10] Schulze, H., Schuler, A., Stuber, D., Dobeli, H., Langen, H. and Huber, G. (1993) Rat brain glyceraldehyde-3-phosphate dehydrogenase interacts with the recombinant cytoplasmic domain of Alzheimer's beta-amyloid precursor protein. J. Neurochem. 60, 1915–1922.
[11] Oyama, R., Yamamoto, H. and Titani, K. (2000) Glutamine synthetase, hemoglobin alpha-chain, and macrophage migration inhibitory factor binding to amyloid beta-protein: their identification in rat brain by a novel affinity chromatography and in Alzheimer's disease brain by immunoprecipitation. Biochim. Biophys. Acta 1479, 91–102.
[12] Nakajima, H., Amano, W., Fujita, A., Fukuhara, A., Azuma, Y.T., Hata, F., Inui, T. and Takeuchi, T. (2007) The active site cysteine of the proapoptotic protein glyceraldehyde-3-phosphate dehydrogenase is essential in oxidative stress-induced aggregation and cell death. J. Biol. Chem. 282, 26562–26574.
[13] Zhao, H., Tuominen, E.K. and Kinnunen, P.K. (2004) Formation of amyloid fibers triggered by phosphatidylserine-containing membranes. Biochemistry 43, 10302–10307.
[14] Finer, E.G., Flook, A.G. and Hauser, H. (1972) Mechanism of sonication of aqueous egg yolk lecithin dispersions and nature of the resultant particles. Biochim. Biophys. Acta 260, 49–58.
[15] Susi, H. and Byler, D.M. (1986) Resolution-enhanced Fourier transform infrared spectroscopy of enzymes. Meth. Enzymol. 130, 290–311.
[16] Barksdale, A.D. and Rosenberg, A. (1982) Acquisition and interpretation of hydrogen exchange data from peptides, polymers, and proteins. Meth. Biochem. Anal. 28, 1–113.

[17] LeVine 3rd., H. (1993) Thioflavine T interaction with synthetic Alzheimer's disease beta-amyloid peptides: detection of amyloid aggregation in solution. Protein Sci. 2, 404–410.
[18] Arrondo, J.L., Castresana, J., Valpuesta, J.M. and Goni, F.M. (1994) Structure and thermal denaturation of crystalline and noncrystalline cytochrome oxidase as studied by infrared spectroscopy. Biochemistry 33, 11650–11655.
[19] Echabe, I., Encinar, J.A. and Arrondo, J.L.R. (1997) Removal of spectral noise in the quantitation of protein structure through infrared band decomposition. Biospectroscopy 3, 469–475.
[20] Kim, K.S., Fuchs, J.A. and Woodward, C.K. (1993) Hydrogen exchange identifies native-state motional domains important in protein folding. Biochemistry 32, 9600–9608.
[21] de Jongh, H.H., Goormaghtigh, E. and Ruysschaert, J.M. (1995) Tertiary stability of native and methionine-80 modified cytochrome *c* detected by proton–deuterium exchange using on-line Fourier transform infrared spectroscopy. Biochemistry 34, 172–179.
[22] Arrondo, J.L., Muga, A., Castresana, J. and Goni, F.M. (1993) Quantitative studies of the structure of proteins in solution by Fourier-transform infrared spectroscopy. Prog. Biophys. Mol. Biol. 59, 23–56.
[23] Byler, D.M. and Susi, H. (1986) Examination of the secondary structure of proteins by deconvolved FTIR spectra. Biopolymers 25, 469–487.
[24] Krimm, S. and Bandekar, J. (1986) Vibrational spectroscopy and conformation of peptides, polypeptides, and proteins. Adv. Protein Chem. 38, 181–364.
[25] Cowan-Jacob, S.W., Kaufmann, M., Anselmo, A.N., Stark, W. and Grutter, M.G. (2003) Structure of rabbit-muscle glyceraldehyde-3-phosphate dehydrogenase. Acta Crystallogr. D Biol. Crystallogr. 59, 2218–2227.
[26] Arrondo, J.L., Young, N.M. and Mantsch, H.H. (1988) The solution structure of concanavalin A probed by FT-IR spectroscopy. Biochim. Biophys. Acta 952, 261–268.
[27] Markossian, K.A. et al. (2006) Mechanism of thermal aggregation of rabbit muscle glyceraldehyde-3-phosphate dehydrogenase. Biochemistry 45, 13375–13384.
[28] Mazzola, J.L. and Sirover, M.A. (2002) Alteration of intracellular structure and function of glyceraldehyde-3-phosphate dehydrogenase: a common phenotype of neurodegenerative disorders? Neurotoxicology 23, 603–609.
[29] Naletova, I., Schmalhausen, E., Kharitonov, A., Katrukha, A., Saso, L., Caprioli, A. and Muronetz, V. (2008) Non-native glyceraldehyde-3-phosphate dehydrogenase can be an intrinsic component of amyloid structures. Biochim. Biophys. Acta 1784, 2052–2058.
[30] Ferrone, F. (1999) Analysis of protein aggregation kinetics. Meth. Enzymol. 309, 256–274.
[31] Avila, C.L., de Arcuri, B.F., Gonzalez-Nilo, F., De Las Rivas, J., Chehin, R. and Morero, R. (2008) Role of electrostatics on membrane binding, aggregation and destabilization induced by NAD(P)H dehydrogenases. Implication in membrane fusion. Biophys. Chem. 137, 126–132.
[32] de la Fuente, M. and Ossa, C.G. (1997) Binding to phosphatidyl serine membranes causes a conformational change in the concave face of annexin I. Biophys. J. 72, 383–387.
[33] Mockrin, S.C., Byers, L.D. and Koshland Jr., D.E. (1975) Subunit interactions in yeast glyceraldehyde-3-phosphate dehydrogenase. Biochemistry 14, 5428–5437.
[34] Kelly, J.W. (1998) The alternative conformations of amyloidogenic proteins and their multi-step assembly pathways. Curr. Opin. Struct. Biol. 8, 101–106.
[35] Uversky, V.N. and Fink, A.L. (2004) Conformational constraints for amyloid fibrillation: the importance of being unfolded. Biochim. Biophys. Acta 1698, 131–153.